Solvent Quality Changes the Structure of G8 PAMAM Dendrimer, a Disagreement with Some Experimental Interpretations

Prabal K. Maiti*,† and William A. Goddard III‡

Center for Condensed Matter Theory and Department of Physics, Indian Institute of Science, Bangalore 560012, and Materials and Process Simulation Center, California Institute of Technology, Pasadena, California 91125

Received: April 12, 2006; In Final Form: October 3, 2006

We have performed ∼20−40 ns of molecular dynamics (MD) simulations for the generation 8 PAMAM dendrimer in explicit water under varying pH conditions to study the structure of the dendrimer (∼156 738 atoms at low pH). This is the first report of such a long MD simulation of a larger generation PAMAM dendrimer including the effect of salt and counterions with explicit water molecules. We find that changing the pH from a high value (∼12) to a low value (∼3) changes the radius of gyration from $R_g = 37.8$ to 43.1 Å (increasing by 13%). We also find significant back-folding of the primary amines and a large amount of water penetration inside the polymer. The increase in size with decrease in pH is consistent with our earlier studies on G3−G6 and agrees with the Monte Carlo theory by Welch and Muthukumar of G8 (*Macromolecules*, **1998**, *31*, 5892) and the experiments on G5 and G8 PAMAM dendrimer by Topp et al. (*Macromolecules*, **1999**, *32*, 7232). However, these results disagree dramatically with the interpretations of SANS experiments of G8 PAMAM dendrimers by Nisato et al. (*Macromolecules*, **2000**, *33*, 4172) who observe no change in the size of the dendrimer with variations of solution pH and ionic strength. We assume that the disagreement might arise from neglecting nonspherical shape, penetration of water and ions into the core, and aggregation, all of which might depend on pH.

Dendritic polymers or dendrimers are synthesized using a stepwise repetitive reaction sequence that guarantees a very highly monodisperse polymer, leading to a nearly perfect hyperbranched topology radiating from a central core (see Figure 1). These macromolecules have a unique combination of properties, such as size, shape, surface/interior chemistry, flexibility, and topology, providing solutions for applications ranging from drug delivery[1,2] to molecular encapsulation[3,4] and gene therapy,[5] from building blocks for nanostructures to micelle mimics as decontaminating agents.[6] Particularly interesting is the unique pH-responsive behavior of PAMAM dendrimer under varying solution conditions. The ability to control the physiochemical properties of the dendrimer by changing solution pH is key to such applications as drug delivery and gene therapy. The size of the dendrimers also depends on the solvent quality, but recently a disagreement concerning the magnitude and sign has arisen.[7,8] Small-angle neutron scattering experiments (SANS) in dilute solutions of $D(CD_2)_mOD$ (with $m = 0, 1, 2, 4$) show[7] that with decreasing solvent quality (decrease of the polarity of the solvent) the radius of gyration of PAMAM dendrimers of generation 5 and 8 decreases by ∼10%. However, these findings are contradicted the experiments of Nisato et al.,[9] who used small-angle neutron scattering to study the effect of ionic strength and pH on conformational changes of generation 8 PAMAM dendrimer in D_2O. Nisato et al. observed that the size of the generation 8 PAMAM dendrimer is insensitive to the variations of pH. This is contrary to the results from Monte Carlo (MC) simulation studies by Welch and Muthukumar,[10] who predicted a nearly 180% *increase* in dendrimer size as the ionic concentration and pH of the solvent are changed from very high to very low (Debye length was increased from 3 to 300 Å).

To resolve this clear conflict between the theory and experiment and between experiments we report here detailed molecular dynamics (MD) simulations of G8 PAMAM dendrimers with explicitly included solvent and counterions (all previous simulations of G8 ignored explicit solvent and ions). We consider a variety of pH conditions in explicit water. Our earlier MD simulations of G4−G6 PAMAM dendrimers in explicit salt water showed a 33% increase in the size of the dendrimer for changes in the solution from pH = 12 to 4.[11] Our new simulations address the questions as to whether the phenomena of charge-induced swelling of dendrimer is a generic phenomena for all the generations or is limited only to lower generations.[12]

The details of the building of the atomic model of various generations of PAMAM dendrimers at various protonation levels are published elsewhere.[11,13] To mimic the targeted pH conditions, we carried out simulations at three protonation levels:

- High pH: no protonation (pH > 12).
- Intermediate or neutral pH: all 1024 primary amines are protonated, but none of the tertiary amines are protonated (pH ∼ 7).
- Low pH: all 1024 primary amines and 1022 tertiary amines are protonated (pH < 4).

The above pH conventions was motivated by the potentiometric titration studies,[14] which demonstrated that at high pH (∼1) none of the primary and tertiary amines are protonated, at neutral pH (∼7) almost all the primary amines are protonated, and at low pH (∼4) all the tertiary amines are also protonated. Similar conventions were used in the work of Baker and co-

† Indian Institute of Science. E-mail: maiti@physics.iisc.ernet.in.
‡ California Institute of Technology. E-mail: wag@wag.caltech.edu.

10.1021/jp0622684 CCC: $33.50 © 2006 American Chemical Society
Published on Web 11/30/2006

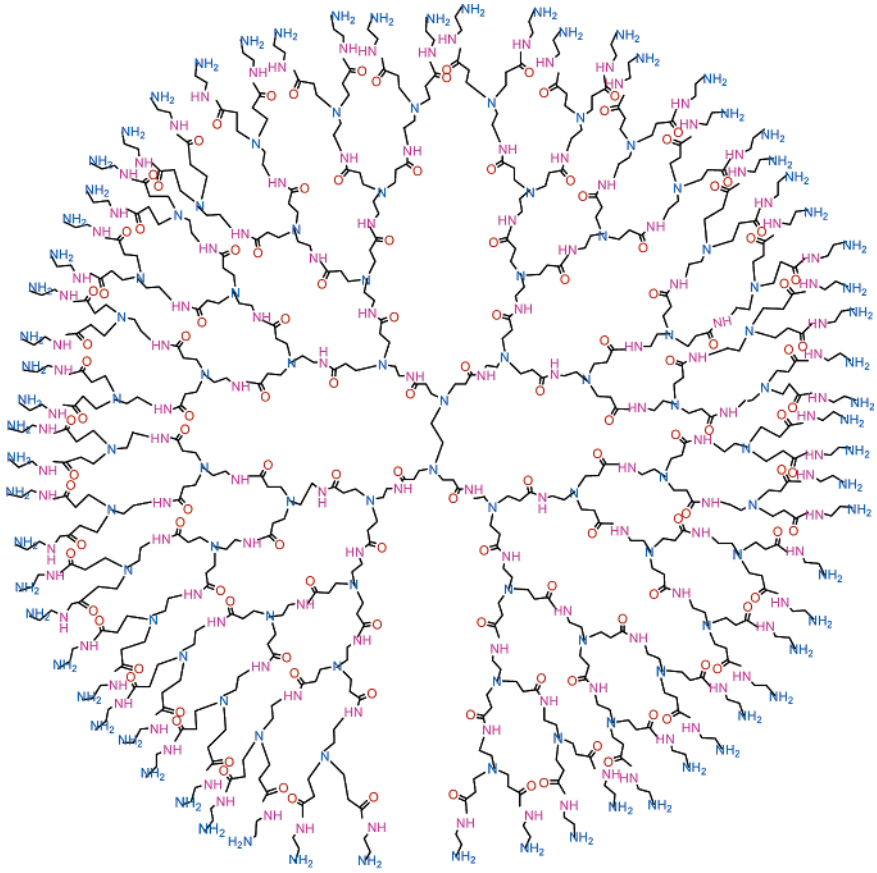

Figure 1. Two-dimensional schematic representation of fourth generation (64 primary and 62 tertiary amine sites) PAMAM dendrimer.

workers who reported the effect of pH on the structure and dynamics of generations G2−G5 PAMAM dendrimer in both implicit solvent[15] and in explicit solvent.[16]

Our calculations used the LEAP module in AMBER,[17] to immerse various protonation levels of the G8 PAMAM dendrimer in a periodic water box, with the waters described using the TIP3P force field (FF). To reduce the number of water molecules required we used a truncated octahedral box (bcc) with a cell length of 116 Å. The box dimensions were chosen to ensure at least a 10 Å solvation shell around the dendrimer structure.

For the high pH, the dendrimer is neutral and no counterions are needed. However, to describe the neutral and low-pH cases, the appropriate number of waters were replaced by Cl^- counterions to neutralize the positive charge on the protonated primary and tertiary amine sites on the dendrimer structures. This procedure resulted in solvated G8 dendrimer structures, containing 120 750 atoms for high pH, 120 770 atoms for neutral pH, and 156 738 atoms for low pH.

MD simulation was performed using the AMBER7[17] software suite with the Dreiding force field.[18] The solvated structures were subjected to 1000 steps of steepest descent minimization of potential energy, followed by another 2000 steps of conjugate gradient minimization. During this minimization the dendrimer structure was kept fixed in its starting conformations using a harmonic constraint with a force constant of 500 kcal/mol/Å^2. This allowed the reorganization of the water molecules to eliminate bad contacts with the dendrimer structure. The minimized structure was then subjected to 45 ps of MD, with a 2 fs time step. During the dynamics, the system was gradually heated (over 40 ps) from 0 to 300 K with harmonic constraints on the solute using the SHAKE method. This was followed by 200 ps constant volume−constant temperature (NVT) dynamics with a temperature coupling constant of 0.5−1.0 ps on the solute. Finally, ∼20−40 ns NPT unrestrained production dynamics was carried out using a time constant of 1 ps for heat bath coupling. This long time was required to fully equilibrate the system (see Figure S1 in the Supporting Information). The electrostatics interactions were evaluated with the particle mesh Ewald[19] (PME) method, using a real space cutoff of 9 Å. A similar method used in our recent study on poly(propyl ether imine) (PETIM) dendrimer[20] yields a size estimate of the dendrimer in quantitative agreement with SAXS data. The salt concentration in our simulation corresponds to a Debye length of 11 Å for neutral pH and 14 Å for low pH, representing the case of high salt concentration.

A quantitative estimate of the dendrimer shape and size is given by the mean-square radius of gyration $\langle R_g^2 \rangle$ and shape tensor of the individual chain. For a dendrimer with N atoms the mean-square radius of gyration is $\langle R_g^2 \rangle = (1/M)\langle [\sum_{i=1}^{N} m_i|r_i - R|^2] \rangle$, where R is the center-of-mass of the dendrimer, r_i and m_i are the position and mass of the ith atom, and M is the total mass of the dendrimer.

Figure 2 shows the radius of gyration R_g for G8 PAMAM at different protonation levels. *We see a nearly 13% increase in size on going from pH=12 to pH = 4.*

Figure 2 also shows the size of the G8 PAMAM determined experimentally by Nisato et al. using small-angle neutron scattering (SANS) at three different pH levels. These experiments dissolved G8 PAMAM in D_2O solution and varied the pH of the dendrimer solution from 4 to 10 by adding a small concentration of HCl or NaOH solution. In dramatic disagreement with our simulations and those of others and with previous experiments on G5 and G8 PAMAM dendrimer by Topp et al.,[7] Nisato et al. find no dependence on solution pH.

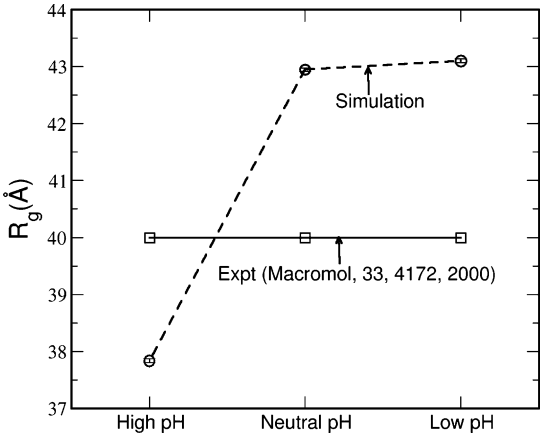

Figure 2. Predicted radius of gyration (R_g) of G8 PAMAM at various pH levels. We find a 13% size increase in going from high pH (~12) to neutral pH (~7). The calculated values of R_g from our simulation are 37.8 ± 0.03 Å (high pH), 42.9 ± 0.02 Å (neutral pH), and 43.11 ± 0.03 Å. The dotted line is a guide the eye. In contrast, the experiments of Nisato et al.[9] are interpreted to find no changes in size. The experimental R_g values from Nisato et al. are 39.1 Å (high pH), 39.6 Å (neutral pH), and 40.7 Å (low pH).

The origin of this swelling is the favorable interaction of the solvent with the primary and tertiary amines. Thus, our simulations (in the presence of water) find significant penetration of water throughout the interior of the dendrimer, causing a swelling of the dendrimer structure. Protonating the amines, particularly the tertiary amines inside the dendrimer, brings additional water into the dendrimer, leading to additional swelling (arising from both the excluded volume interactions and the Coulombic repulsions between the protonated primary and tertiary amines). However, for G8 this increase in size is 10%, much smaller than for lower generation PAMAM where we found a 33% increase in size for G4, G5, and G6 on going from high to low pH.[21] Our rationale for this difference is that for G8 the interior of the dendrimer is already very crowded, leaving less space to accommodate additional water and ions. This was shown in earlier vacuum phase simulations for PAMAM dendrimers up to G11,[13] where we found a marked increase in internal strain above G8.

Recently Terao et al.[22] studied the pH dependence on smaller generation model dendrimers (up to G7) using stochastic molecular dynamics simulation. Using a short spacer length for G7 dendrimer, they observe no size change as a function of pH. This might seem inconsistent with our PAMAM simulations; however, their short spacer is far too small to represent PAMAM, and it is plausible that steric hindrance will dominate, since the branches have little conformational freedom.

Also, recent MD studies on charged dendrimer using a coarse-grained model[23] demonstrate that inclusion of explicit counterion is very crucial and cannot be treated implicitly. The use of the Debye−Hückel approximation for charged dendrimers (as in the work by Terao at. al) may not be reliable.

It is also possible that changing the FF might change the coordination numbers for water and ion[24] which affect the degree of swelling. However, our studies have used both the F3C and TIP3P models of water and find similar effects.

We find that the presence of counterions contributes to the swelling. Increasing the degree of protonation has a significant effect on the number of counterions condensed within the dendrimer. These reside close to the protonated sites while being solvated the waters, resulting in an increase in osmotic pressure. As the protonation level increases from pH = 7 to pH = 4, the fraction of counterions inside the dendrimer solvent accessible surface increases from 65% to79%, leading to increased swelling.

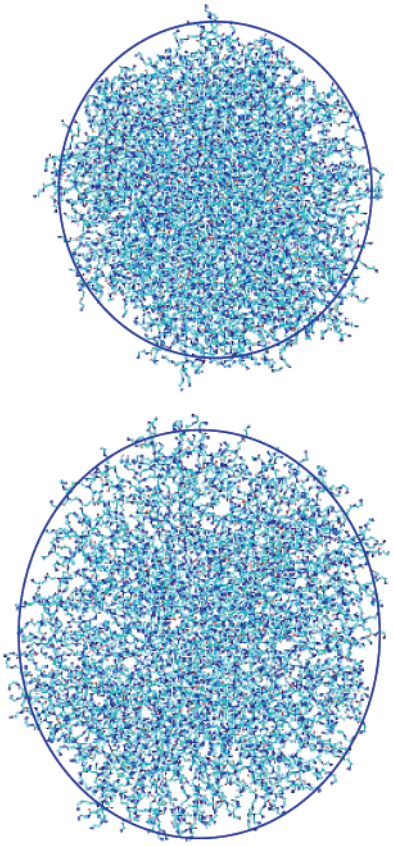

Figure 3. Snapshot of PAMAM dendrimer at high and low pH. The size changes by 13% in going from high to low pH. The shape also changes: (I_z/I_y) changes from 1.2 at neutral pH to 1.4 at low pH. (I_z/I_x) goes from 1.8 at high pH to 1.95 at low pH. These snapshots were generated using the VMD software (ref 31) developed at UIUC.

The aspect ratio of the three principal moments of inertia, (I_z/I_y) and (I_z/I_x), were calculated to characterize the shape anisotropy of the dendrimer (here $I_z > I_y > I_x$). We find that (I_z/I_y) changes from 1.4 at high pH to 1.2 at neutral pH, and back to 1.4 again at low pH. Similarly, (I_z/I_x) goes from 2.3 to 1.8 to 1.9 on going from high pH to neutral to low pH. This indicates that the G8 PAMAM in solution has the shape of an oblate ellipsoid, which is consistent with the dendrimer shape observed in TEM and AFM experiments on G8 PAMAM dendrimer.[25,26] This change in shape is shown in Figure 3, with a snapshot of the final configuration for G8 at high and low pH levels.

Figure 4a shows the effect of pH on the radial monomer density for G8 PAMAM. For high pH the density achieves its maximum in the middle of the dendrimer (~20 Å from the center-of-mass), leading to a large region with constant density. However, at low pH this feature disappears, leading to a maximum density near the center of the molecule (~10 Å from the center-of-mass) and decays toward the edge of the molecule. This is indicating that the core region is denser than the middle of the dendrimer, which is fairly hollow. These results support the de Gennes model[27,28] and are consistent with previous Monte Carlo simulations and theoretical predictions by Welch and Muthukumar.[10] Due to this hollowness in the middle region of the dendrimer, a significant number of waters penetrate to the middle of the dendrimer. The water density profiles in Figure 4a support this picture. As the dendrimer size increases due to

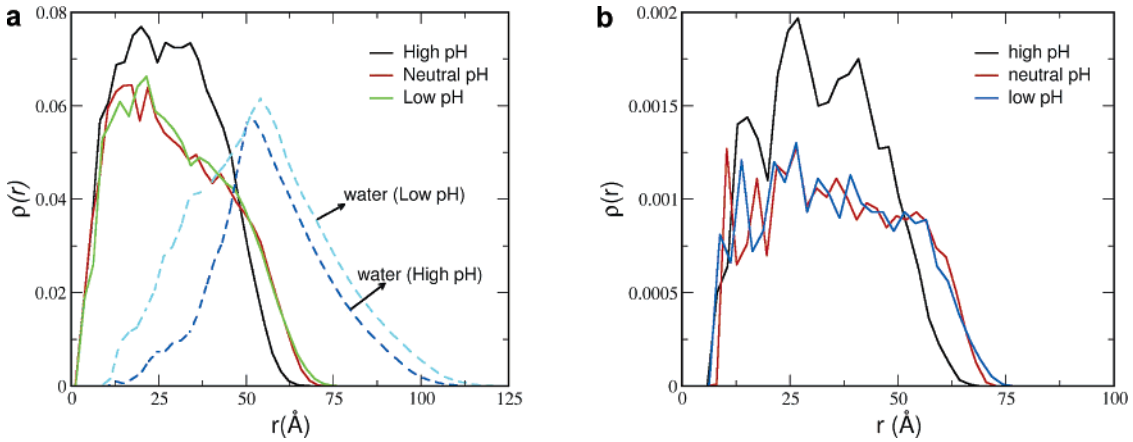

Figure 4. (a) Radial monomer densities for G8 PAMAM dendrimers at three pH conditions. The numbers shown were averaged over the trajectory from 1 to 20 ns, using snapshots every 0.5 ps. The origin is at the center-of-mass. We see a significant degree of water penetration inside the dendrimer for both high pH and low pH values. (b) Radial monomer density distribution of the primary nitrogens at various solvent conditions. This shows significant back-folding for all pH values, with the degree of back-folding decreasing as the pH is decreased.

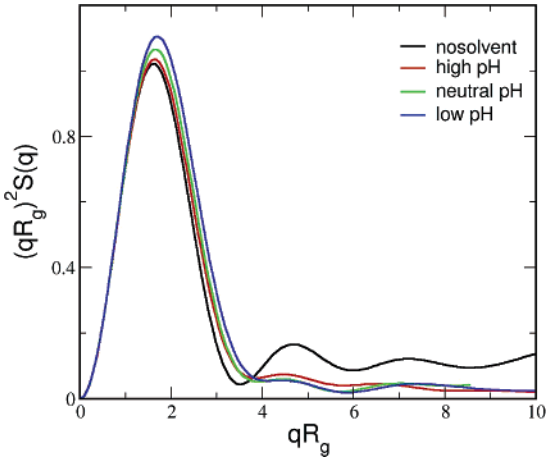

Figure 5. Single-particle form factor in the Kratky representation for various pH values. The minima shift to lower q values for low pH indicating the swelling of the dendrimer.

the swelling, the density profile extends more radially outward compared to that of the unprotonated case at high pH. Figure 4b shows the density profile for the terminal nitrogens at three pH levels. This indicates that the end-groups of different subgenerations of a given dendrimer are sufficiently flexible to interpenetrate throughout nearly the whole molecule. The terminal groups are no longer all located at the periphery of the molecule. Instead, some come close to the core of the molecule (back-folded). In going from high pH to low pH there is a reduction in the degree of back-folding due to strong electrostatic repulsion between the charged amine groups.

The single-particle form factors in the Kratky representation are shown for three pH conditions in Figure 5. For comparison, we also show the form factor for the case with no solvent, where we see that the lack of solvent leads to a more compact structure. With an increase in protonation (lower pH) an internal ordering develops inside the dendrimer, which helps sharpen the secondary peaks for low pH compared to the high-pH case. This is consistent with the shape anisotropy calculations described in the previous section. The positions of the first minima in the scattering curves yield the overall size of the dendrimer. Figure 5 shows that the position of the first minima shifts to a lower q value (indicating an increase in size) as pH is decreased.

For comparison, Figure 2 also shows the size of the G8 PAMAM determined experimentally using SANS at three different pH levels. These SANS experiments find no dependence on solution pH, in clear disagreement with the simulations. All theoretical models agree at least qualitatively that lower pH leads to larger sizes. We do not have a convincing explanation for this discrepancy with experiment. Possibly it might arise from the assumption of a spherical shape in extracting size from the SANS data. Our new simulations and all previous ones find an asymmetric shape. In addition, recent determination of shape from SANS and SAXS experiments on polycarbosilane dendrimers shows that generation G8−G9 dendrimers have very large shape anisotropy (ratios of $a/b/c = 2.3:1.6:1$).[29] In addition, the experimental interpretation does not account for the significant water and counterion content in the interior of the dendrimer (evident in Figure 4). Another possibility might involve corrections for dendrimer aggregation in the experiment. Additional experiments aimed at taking into consideration aggregation and dendrimer shape would be useful. Possibly, NMR experiments to determine the chemical shifts as a function of pH would help resolve the discrepancy.

Summarizing, this is the first report of such long MD of a larger generation PAMAM dendrimer solvated in explicit water molecules and including the effect of salt and counterions. We conclude from ∼20−40 ns of atomistic MD simulation that decreasing solvent pH from 10 to 4 has a significant effect (13%) on the size of G8 PAMAM dendrimer. This agrees with our previous simulations on lower generation (G4−G6) PAMAM dendrimer,[21] which found even larger effects (33%). These works conclusively demonstrate that the charge-induced phenomenon of swelling is a generic phenomenon in PAMAM dendrimer. This significant swelling at low pH results from incorporation of solvent and ions to solvate the protonated tertiary amines, leading to larger amount of water inside the dendrimer that can facilitate metal ion binding. These results are in stark contrast with interpretations of recent SANS experiment on the G8 PAMAM dendrimer. We assume that this discrepancy arises from assumptions in reducing the data to obtain a size (spherical shape, ignoring solvent and ions in the interior, and ignoring dendrimer aggregation).

We also find significant back-folding of the primary amines into the interior of the dendrimer and large amounts of water penetrating the polymer. The aspect ratio of the dendrimer at all the pH values shows that the dendrimer is best approximated as an oblate ellipsoidal. This agrees with recent AFM studies on G8 PAMAM dendrimer.[30]

Acknowledgment. We thank the Supercomputer Education and Research Center (SERC) and the Center for High-Energy Physics (CHEP), IISc, Bangalore for providing generous computer time where all the computations have been carried out. P.K.M. thanks DST (India) for financial support. Our simulations on dendrimers were initiated with funding from an ARO-MURI (Kiserow) and were continued with funding from NSF.

Supporting Information Available: Time evolution of the radius of gyration at various protonation levels showing the equilibration period and a figure showing the radial monomer density profile at low pH including the contribution coming from each sub generations. We also show the solvent excluded surface area at various pH conditions. This material is available free of charge via the Internet at http://pubs.acs.org.

References and Notes

(1) Haensler, J.; Szoka, F. C. *Bioconjugate Chem.* **1993**, *4*, 372.
(2) Bielinska, A.; KukowskaLatallo, J. F.; Johnson, J.; Tomalia, D. A.; Baker, J. R. *Nucleic Acids Res.* **1996**, *24*, 2176.
(3) Jansen, J.; Debrabandervandenberg, E. M. M.; Meijer, E. W. *Science* **1994**, *266*, 1226.
(4) Miklis, P.; Cagin, T.; Goddard, W. A. *J. Am. Chem. Soc.* **1997**, *119*, 7458.
(5) Tang, M. X.; Redemann, C. T.; Szoka, F. C. *Bioconjugate Chem.* **1996**, *7*, 703.
(6) Bosman, A. W.; Janssen, H. M.; Meijer, E. W. *Chem. Rev.* **1999**, *99*, 1665.
(7) Topp, A.; Bauer, B. J.; Tomalia, D. A.; Amis, E. J. *Macromolecules* **1999**, *32*, 7232.
(8) Stechemesser, S. E. W. *Macromolecules* **1999**, *32*, 7232.
(9) Nisato, G.; Ivkov, R.; Amis, E. J. *Macromolecules* **2000**, *33*, 4172.
(10) Welch, P.; Muthukumar, M. *Macromolecules* **1998**, *31*, 5892.
(11) Lin, S. T.; Maiti, P. K.; Goddard, W. A. *J. Phys. Chem. B* **2005**, *109*, 8663.
(12) Ballauff, M.; Likos, C. N. *Angew. Chem.* **2004**, *43*, 2998.
(13) Maiti, P. K.; Cagin, T.; Wang, G. F.; Goddard, W. A. *Macromolecules* **2004**, *37*, 6236.
(14) Cakara, D.; Kleimann, J.; Borkovec, M. *Macromolecules* **2003**, *36*, 4201.
(15) Lee, I.; Athey, B. D.; Wetzel, A. W.; Meixner, W.; Baker, J. R. *Macromolecules* **2002**, *35*, 4510.
(16) Lee, H.; Baker, J. R.; Larson, R. G. *J. Phys. Chem. B* **2006**, *110*, 4014.
(17) Case, D. A.; Pearlman, D. A.; Caldwell, J. W.; Cheatham, T. E.; Wang, J.; Ross, W. S.; Simmerling, C.; Darden, T.; Merz, K. M.; Stanton, R. V.; et al. *AMBER7*, 7th ed.; University of California: San Francisco, CA, 1999.
(18) Mayo, S. L.; Olafson, B. D.; Goddard, W. A. *J. Phys. Chem.* **1990**, *94*, 8897.
(19) Darden, T.; York, D.; Pedersen, L. *J. Chem. Phys.* **1993**, *98*, 10089.
(20) Jana, C.; Jayamurugan, G.; Ganapathy, R.; Maiti, P. K.; Jayaraman, N.; Sood, A. K. *J. Chem. Phys.* **2006**, *124*.
(21) Maiti, P. K.; Cagin, T.; Lin, S. T.; Goddard, W. A. *Macromolecules* **2005**, *38*, 979.
(22) Terao, T.; Nakayama, T. *Macromolecules* **2004**, *37*, 4686.
(23) Gurtovenko, A. A.; Lyulin, S. V.; Karttunen, M.; Vattulainen, I. *J. Chem. Phys.* **2006**, *124*, 094904.
(24) Patra, M.; Karttunen, M. *J. Comput. Chem.* **2004**, *25*, 678.
(25) Li, J.; Piehler, L. T.; Qin, D.; Baker, J. R.; Tomalia, D. A.; Meier, D. J. *Langmuir* **2000**, *16*, 5613.
(26) Jackson, C. L.; Chanzy, H. D.; Booy, F. P.; Drake, B. J.; Tomalia, D. A.; Bauer, B. J.; Amis, E. J. *Macromolecules* **1998**, *31*, 6259.
(27) Zook, T. C.; Pickett, G. T. *Phys. Rev. Lett.* **2003**, *90*.
(28) de Gennes, P. G.; Hervet, H. *J. Phys. Lett.* **1983**, *44*, L351.
(29) Ozerin, A. N.; Svergun, D. I.; Volkov, V. V.; Kuklin, A. I.; Gordeliy, V. I.; Islamov, A. K.; Ozerina, L. A.; Zavorotnyuk, D. S. *J. Appl. Crystallogr.* **2005**, *38*, 996.
(30) Camara, R. P.; Papastavrou, G.; Borkovec, M. *Langmuir* **2004**, *20*, 3264.
(31) Humphrey, W.; Dalke, A.; Schulten, K. *J. Mol. Graphics* **1996**, *14*, 33.